HHS Public Access

Author manuscript

J Invest Dermatol. Author manuscript; available in PMC 2016 July 01.

Published in final edited form as:

J Invest Dermatol. 2016 January ; 136(1): 59–66. doi:10.1038/JID.2015.353.

Super-resolution microscopy reveals altered desmosomal protein organization in pemphigus vulgaris patient tissue

Sara N. Stahley[1,2], **Maxine F. Warren**[1], **Ron J. Feldman**[3], **Robert A. Swerlick**[3], **Alexa L. Mattheyses**[1], and **Andrew P. Kowalczyk**[1,3,4]

[1] Department of Cell Biology, Emory University School of Medicine, Atlanta, Georgia, United States of America

[2] Graduate Program in Biochemistry, Cell and Developmental Biology, Emory University School of Medicine, Atlanta, Georgia, United States of America

[3] Department of Dermatology, Emory University School of Medicine, Atlanta, Georgia, United States of America

[4] Winship Cancer Institute, Emory University School of Medicine, Atlanta, Georgia, United States of America

Abstract

Pemphigus vulgaris (PV) is an autoimmune epidermal blistering disease in which autoantibodies (IgG) are directed against the desmosomal cadherin desmoglein 3 (Dsg3). In order to better understand how PV IgG alters desmosome morphology and function *in vivo*, PV patient biopsies were analyzed by structured illumination microscopy (SIM), a form of super-resolution fluorescence microscopy. In patient tissue, desmosomal proteins were aberrantly clustered and localized to PV IgG-containing endocytic linear arrays. Patient IgG also colocalized with markers for lipid rafts and endosomes. Additionally, steady-state levels of Dsg3 were decreased and desmosomes were reduced in size in patient tissue. Desmosomes at blister sites were occasionally split, with PV IgG decorating the extracellular faces of split desmosomes. Desmosome splitting was recapitulated in vitro by exposing cultured keratinocytes both to PV IgG and to mechanical stress, demonstrating that splitting at the blister interface in patient tissue is due to compromised desmosomal adhesive function. These findings indicate that Dsg3 clustering and endocytosis are associated with reduced desmosome size and adhesion defects in PV patient tissue. Further, this study reveals that super-resolution optical imaging is powerful approach for studying epidermal adhesion structures in normal and diseased skin.

Address correspondence to: Andrew P. Kowalczyk, Department of Cell Biology, Emory University, 615 Michael Street, Atlanta, Georgia 30322, USA, Tel: 404-727-8517, Fax: 404-727-6256, akowalc@emory.edu.

CONFLICT OF INTEREST

The authors state no conflict of interest.

INTRODUCTION

The desmosome is an intercellular junction that mediates robust adhesion between neighboring cells (Berika and Garrod, 2014; Kowalczyk and Green, 2013). Desmosomes are present in all epithelia, but are especially prominent in the skin and the heart (Berika and Garrod, 2014; Desai *et al.*, 2009). These tissues experience a high degree of mechanical stress, and for this reason, desmosome dysfunction leads to skin and heart defects that are often characterized by tissue fragility (Al-Jassar *et al.*, 2013; Cirillo, 2014; Kottke *et al.*, 2006; Thomason *et al.*, 2010). Desmosomes comprise desmosomal cadherins, which engage in extracellular adhesive interactions, and cytoplasmic plaque proteins, including plakoglobin, plakophilin and desmoplakin (DP), which mediate linkages to the intermediate filament cytoskeleton. Desmogleins (Dsg) and desmocollins (Dsc) are desmosomal transmembrane proteins and members of the cadherin superfamily of adhesion molecules. The armadillo family protein plakoglobin links the cytoplasmic tail of the cadherins to DP, an intermediate filament binding protein and member of the plakin family of cytolinkers. Plakophilin, also an armadillo protein, facilitates lateral interactions between desmosomal cadherin complexes and further strengthens the plaque (Desai *et al.*, 2009; Kowalczyk and Green, 2013). This architectural arrangement couples desmosomal cadherin adhesive interactions to the intermediate filament cytoskeleton, thereby establishing an integrated adhesive and cytoskeletal network that extends throughout a tissue (Kowalczyk and Green, 2013).

Desmosome assembly and disassembly dynamics must be precisely controlled to allow not only for strong adhesion and tissue integrity, but also for plasticity during processes such as wound healing and development (Nekrasova and Green, 2013). Alterations in desmosome dynamics are thought to contribute to desmosome disruption and loss of adhesion in disease states, including the autoimmune blistering disease pemphigus vulgaris (PV) (Kitajima, 2013, 2014). Pemphigus is a family of potentially fatal bullous diseases caused by autoantibodies directed against the extracellular domain of desmosomal cadherins (Amagai, 2009, 2010). Patients with PV produce IgG autoantibodies that target Dsg3, or both Dsg3 and Dsg1 (Amagai, 2009). PV IgG binding to the desmosomal cadherins results in the loss of keratinocyte adhesion, termed acantholysis, between the basal and spinous layers of the epidermis (Amagai, 2010). Clinically, the disease presents as painful mucosal erosions and epidermal blisters (Kneisel and Hertl, 2011). Although it has been established that anti-Dsg3 antibodies are sufficient to cause disease, the precise pathomechanisms by which PV IgG cause loss of adhesion and blister formation are not fully understood.

Much of what we know about PV pathomechanisms comes from *in vitro* work in which cultured keratinocytes are exposed to PV IgG. Previous experiments by our group and others using cell culture models have revealed that PV IgG cause aberrant clustering of cell surface Dsg3, leading to increased endocytosis and decreased steady state levels of Dsg3 (Calkins *et al.*, 2006; Iwatsuki *et al.*, 1999; Iwatsuki *et al.*, 1989; Jolly *et al.*, 2010; Mao *et al.*, 2014; Mao *et al.*, 2011; Patel *et al.*, 1984; Saito *et al.*, 2012; Sato *et al.*, 2000). In response to PV IgG *in vitro*, Dsg3 and other desmosomal components rearrange into streaks, or linear arrays, which extend perpendicularly from cell-cell borders (Jennings *et al.*, 2011). These structures appear to be associated with lipid raft mediated endocytosis of the Dsg3-PV IgG

complex (Delva *et al.*, 2008; Stahley *et al.*, 2014). Furthermore, multiple signaling pathways have been implicated in PV pathogenesis, including tyrosine kinases and p38MAPK-dependent pathways, (Getsios *et al.*, 2004; Kitajima, 2014; Koga *et al.*, 2013; Sharma *et al.*, 2007; Waschke, 2008). There is also substantial evidence suggesting that steric hindrance of Dsg3-mediated adhesion causes keratinocyte acantholysis. For example, the majority of IgG isolated from PV patients are directed against the amino terminal domain of Dsg3, a region of cadherins known to mediate adhesion (Amagai *et al.*, 1992; Di Zenzo *et al.*, 2012; Patel *et al.*, 2003; Sekiguchi *et al.*, 2001; Shapiro and Weis, 2009). Further, monoclonal Dsg3 antibodies that target the adhesive interface cause loss of adhesion in cultured keratinocytes and blistering in mouse models of disease (Payne *et al.*, 2005; Tsunoda *et al.*, 2003). In aggregate, these studies suggest that multiple mechanisms, perhaps acting synergistically, contribute to PV pathogenesis. However, previous studies have not directly compared the desmosomal alterations in PV patient skin to those previously observed in cell culture models.

A significant deficit in our understanding of PV pathomechanisms in patients is due to the difficulty in assessing the organization and localization of the desmosomal proteins in multiple patients at high levels of spatial resolution. While electron microscopy provides high resolution ultrastructural information, it is limited by difficult sample preparation, small sample size, and the challenges associated with quantitatively assessing the colocalization of various desmosomal proteins with other cellular antigens. In contrast, optical microscopy approaches such as wide-field and confocal immunofluorescence allow for high throughput of samples and detection of multiple proteins, but lack the spatial resolution sufficient to discern how desmosomal structures are altered in disease states such as PV.

Here, we take advantage of recent advances in optical imaging approaches that bridge the resolution gap between electron microscopy and standard immunofluorescence imaging. Using structured illumination microscopy (SIM), a form of super-resolution optical imaging, we assessed how desmosomes are altered in PV patients. Further, we directly compared the desmosomal alterations observed in PV patients with the PV IgG-induced alterations that occur *in vitro*. Our results indicate that desmosomal protein clustering and Dsg endocytosis occur in patient tissue and that these changes are associated with reduced desmosome size and desmosome splitting at the adhesive interface. We further demonstrate that desmosome splitting can be replicated in cultured keratinocytes by exposing PV IgG treated cells to mechanical stress. These findings reveal new insights into the changes in desmosomal protein organization, trafficking and function that occur in PV patient tissue, and serve to validate the use of purified PV IgG and cultured keratinocytes as an invaluable model system to understand PV pathomechanisms.

RESULTS AND DISCUSSION

PV IgG cause desmosomal protein clustering in patient tissue and in cultured keratinocytes

Desmosomal protein organization in the basal layer of the epidermis of normal human (NH, N1-3) and PV (P1-6) patient tissue was analyzed using structured-illumination microscopy (SIM), a form of super-resolution microscopy that doubles the resolution afforded by

conventional light microscopy (Figure S1). PV patients with clinically active disease and high titers of Dsg3 autoantibodies (Dsg3 ELISA >100) were selected for analysis. Mucocutaneous PV patient tissue was analyzed using biopsies taken from both lip and skin (Table S1).

Biopsies from normal human epidermis were negative for hIgG deposition (Figure 1a, top panel). SIM imaging of NH tissue revealed uniform organization of Dsg3, Dsg1, DP and E-cadherin along cell borders (Figure 1a, top panel). In contrast, PV patient skin exhibited hIgG deposition and disrupted Dsg3, Dsg1 and DP organization (Figure 1a, bottom panel; Figure S3). Importantly, E-cadherin staining remained largely unchanged (Figure 1a, bottom panel). Alterations in junctional protein organization were quantified using a clustering index measuring the average distance between fluorescence puncta along cell borders ((Saito *et al.*, 2012) and Methods). Desmoglein and DP clustering were significantly increased in PV patients, with Dsg3 and DP displaying the greatest alterations relative to controls (Figure 1b; clustering scores from individual patients are displayed in Figure S2). E-cadherin distribution was also altered, although to a lesser degree than observed for desmosomal proteins. The small but statistically significant changes in E-cadherin organization are likely an indirect consequence of desmosome disruption in PV patient skin, since alterations in adherens junctions also have been observed in desmoplakin knock out keratinocytes (Vasioukhin *et al.*, 2001). The organization of plakoglobin also displayed altered organization in PV patient tissue (Supplemental Figure 4). These data support previous observations that desmosomal proteins are clustered in pemphigus patient biopsies (Oktarina *et al.*, 2011). Lastly, we verified that the IgG from each patient analyzed in Figure 1 caused similar alterations in Dsg3 organization *in vitro.* Similar to patient tissue, Dsg3 was clustered in response to IgG from all six PV patients tested (Figure 1c). Collectively, these results demonstrate that clustering of desmosomal proteins is a hallmark feature of both PV IgG treated cells and PV patient tissue.

PV IgG associates with lipid raft markers *in vivo* and is trafficked to endosomes

Previous studies have determined that desmosome disassembly and endocytosis occur in a lipid raft-dependent manner (Delva *et al.*, 2008; Stahley *et al.*, 2014). *In vivo*, patient IgG (hIgG) colocalized with raft markers CD59 and caveolin-1 both at cell borders and in vesicular-like puncta (Figure 2). A number of studies using cell culture models have found that the PV IgG-Dsg complex is internalized from the plasma membrane via lipid raft-mediated endocytosis, resulting in degradation of Dsg3 and reduced plasma membrane levels of the adhesive protein (Calkins *et al.*, 2006; Cirillo *et al.*, 2007; Delva *et al.*, 2008; Jolly *et al.*, 2010; Kitajima, 2014; Mao *et al.*, 2014; Mao *et al.*, 2011; Saito *et al.*, 2012; Sato *et al.*, 2000; Schulze *et al.*, 2012). To determine if PV IgG is internalized to endocytic compartments in patient tissue, biopsy sections were stained for hIgG and the early endosomal marker EEA-1. Nearly every cell, particularly near sites of blister formation, displayed multiple puncta at or near the cell periphery containing hIgG and EEA1 (Figure 3a). Interestingly, steady state Dsg3 levels were decreased in PV patient tissue compared to normal human control tissue (Figure 3b, S5), further suggesting that PV IgG induces Dsg3 endocytosis and degradation *in vivo*.

Desmosomes are smaller and split in PV patients

Ultrastructural studies of desmosome morphology in PV patients and mouse models have suggested that desmosomes either split at the adhesive interface or are reduced in size (Shimizu *et al.*, 2004; van der Wier *et al.*, 2014). We utilized SIM imaging to assess desmosome morphology in patient tissue and directly compared these changes to cultured keratinocytes exposed to patient IgG. We took advantage of information from previous immuno-gold EM studies defining the position of various desmosomal proteins (North *et al.*, 1999) and the sub-diffraction limit resolution of SIM to identify bona fide desmosomes in tissues and cells by immunofluorescence localization. Using this approach, antibodies directed against the carboxyl terminal domain of DP result in a “railroad track” pattern of fluorescence that defines the localization of the inner desmosomal plaque, whereas antibodies against the Dsg extracellular domain identify the adhesive core (Figure 4a-c).

This pattern of DP railroad track staining was used to identify and measure desmosome size in human tissue. Desmosomes in NH samples averaged 0.43 microns in size, while desmosomes in PV patients were significantly smaller, averaging 0.35 microns (Figure 4d,f). This observation is consistent with recent electron microscopy studies of PV patients (van der Wier *et al.*, 2014) and analysis of desmosomes in cultured keratinocytes treated with PV IgG (Saito *et al.*, 2012; Tucker *et al.*, 2014). Interestingly, SIM revealed three types of fluorescence staining patterns in patient tissue (Figure 4b-c, e). First, when DP railroad track staining was intact, we often observed hIgG deposition in the desmosome core (red) that was bracketed by DP staining on opposing keratinocyte membranes (green). Second, a few instances of DP railroad track staining devoid of hIgG deposition in the desmosomal core were also observed, possibly indicating Dsg-depleted desmosomes (Figure S6). Third, we observed numerous split desmosomes in which hIgG was adjacent to only one “rail” of DP (Figure 4e, asterisks), indicating desmosome splitting. The presence of split desmosomes in patients and mouse models of PV has been attributed to pathogenic antibodies physically interfering with, or sterically hindering, desmosomal cadherin adhesive interactions (Amagai *et al.*, 1992; Sharma *et al.*, 2007; Stahley and Kowalczyk, 2015; Tsunoda *et al.*, 2003). If steric hindrance were the sole mechanism for loss of adhesion, we would predict that desmosomes would be split but remain otherwise unchanged morphologically. Interestingly, the majority of split desmosomes in PV patient tissue were also found to be smaller than intact desmosomes in NH tissue (Figure 4f). The observation that desmosomes were often found to be smaller and occasionally depleted of Dsg supports a pathomechanism model for PV that includes altered desmosome assembly or disassembly dynamics.

Mechanical stress causes desmosome splitting

Our analysis of patient tissue using SIM revealed striking similarities in desmosomal protein organization and trafficking in cultured keratinocyte models and PV patient tissue. However, split desmosomes have not been reported in cell culture models of disease, possibly because unlike patient tissue, cultured keratinocytes are not exposed to mechanical stress. To test the hypothesis that mechanical stress causes desmosome splitting, cultured keratinocyte monolayers were subjected to a dispase cell fragmentation assay (Ishii *et al.*, 2005) and then processed for immunofluorescence analysis by SIM. Similar to normal human tissue, the keratinocyte cell sheet exposed to NH IgG remained adhesive and numerous intact

desmosomes were observed (Figure 5). As expected, keratinocytes exposed to PV IgG dissociated upon exposure to mechanical stress. SIM analysis of the free edge of the fragmented cell sheet exposed to PV IgG revealed extensive desmosome splitting (Figure 5) that was strikingly similar to that observed at the blister edge in PV patient biopsies (Figure 4e). These results indicate that the application of mechanical stress causes desmosomes that are weakened by PV IgG to split at the adhesive interface.

Conclusions and Implications

In this study, super-resolution immunofluorescence microscopy revealed changes in desmosomal protein distribution and trafficking that occur in PV patient epidermis. We compared these changes in patient tissue to those that occur in cultured keratinocytes exposed to PV IgG, and have identified hallmark features of the disease that occur both *in vivo* and *in vitro*. In both cases, desmosomal proteins become clustered, enter lipid raft-enriched linear arrays and are internalized to endosomes. These organizational changes are accompanied by a reduction in steady state Dsg3 levels as well as a reduction in desmosome size. Super-resolution imaging also revealed examples of individual desmosomes in patient tissue that were depleted of desmogleins. It is likely that these changes, along with the ability of PV IgG to sterically interfere with desmosomal cadherin adhesion, compromise desmosome function, resulting in mechanical failure upon exposure to mechanical stress. Indeed, desmosome splitting was recapitulated *in vitro* by exposing PV IgG treated keratinocytes to physical forces. Altogether, these results provide further support for a multifactorial model in which PV IgG weaken cell adhesion by altering desmosomal protein distribution, by perturbing the dynamics of desmosome assembly and/or disassembly, and by sterically interfering with desmosome assembly and adhesion (Kitajima, 2013, 2014; Stahley and Kowalczyk, 2015). Finally, this study provides a foundation for using advanced optical imaging techniques to investigate alterations in adhesion structures in a variety of epidermal diseases, and for the development of new optical imaging-based diagnostic metrics for pemphigus and related disorders.

MATERIALS AND METHODS

Human subjects statement

The use of human IgG and skin biopsies was approved by the Institutional Review Board at Emory University. Guidelines set forth in the Declaration of Helsinki were adhered to and written informed consent was obtained from all participants.

Antibodies

The following antibodies were used in this study: mouse anti-Dsg3 antibody AK15 (Tsunoda *et al.*, 2003) was a kind gift from Dr. Masayuki Amagai (Keio University, Tokyo); rabbit anti-desmoplakin antibody NW6 was a kind gift from Dr. Kathleen Green (Northwestern University); mouse anti-Dsg1 antibody P124 (Progen Biotechnik GmbH, Heidelberg); mouse anti-desmoplakin I/II antibody (Fitzgerald, Acton, MA); rabbit anti-γ-catenin (plakoglobin, H-80) and rabbit anti-p120 antibodies (Santa Cruz Biotechnology, Santa Cruz, CA); mouse anti-E-cadherin (HECD-1, Abcam, Cambridge, MA); mouse anti-CD59-FITC conjugated antibody (Invitrogen, Grand Island, NY); rabbit anti-caveolin-1

antibody (BD Biosciences, San Jose, CA); rabbit anti-early endosomal antigen-1 antibody (EEA1) (Thermo Scientific, Waltham, MA). Secondary antibodies conjugated to Alexa Fluors were purchased from Invitrogen. PV sera (used in Figure 5) was a generous gift from Dr. M. Amagai. PV patient sera used in all other Figures were obtained from patients seen at Emory University, Department of Dermatology. IgG was purified from PV sera according to the manufacturer's protocol using Melon Gel IgG Purification Resins and Kits (Thermo Fisher Scientific, Rockford, IL).

Human tissue biopsy processing

Perilesional biopsies (mucosa lip or skin) from six mucocutaneous PV patients seen at the Emory Clinic Dermatology Department were collected and stored at −80°C. 5 μm sections from the biopsies were mounted onto glass slides and processed for immunostaining as described below.

Cells and culture conditions

Primary human keratinocytes (HKs, passage 2 or 4) were isolated as previously described (Calkins *et al.*, 2006) and cultured in KBM-Gold basal medium (100 μM calcium) supplemented with KGM-Gold Single-Quot Kit (Lonza, Walkersville, MD). For Figure 1, HKs were cultured to 70% confluence on glass coverslips and switched to 550 μM calcium 16-18 hrs to induce junction assembly. HKs were exposed to NH IgG or IgG from PV patients for 6 hrs at 37°C, processed for wide-field immunofluorescence and then analyzed for clustering as described below. For the dispase assay in Figure 5, HKs were cultured to 100% confluence in 4-well tissue culture plates and switched to 50 μM calcium to prevent any junction assembly for 16-18 hrs prior to switching to 550 μM calcium for 3 hrs to allow for junction assembly. HKs were exposed to NH or PV IgG for 3hrs at 37°C and processed for a dispase fragmentation assay followed by SIM, as described below.

Immunofluorescence

Patient tissue slices were allowed to come to room temperature and immunostained with primary and secondary antibodies for 1 hr each at room temperature with triple PBS^{+} washes between antibody incubations. HKs in Figure 1 were fixed in methanol and processed for immunofluorescence. Primary antibodies described above and patient IgG present in tissues was detected with Alexa Fluor-conjugated secondary antibodies. Widefield fluorescence microscopy was performed as previously described (Stahley *et al.*, 2014). Super-resolution structured illumination microscopy (SIM) was performed using the N-SIM system equipped with a 100x/1.49 NA oil immersion objective and 488- and 561-nm solid-state lasers. 3D SIM images were captured with an EM charge-coupled device camera (DU-897, Andor Technology, UK) and reconstructed using NIS-Elements software with the N-SIM module (version 3.22, Nikon, Melville, NY). Colocalization analysis via Mander's coefficient was performed using ImageJ Fiji and plugin JACoP (Bolte and Cordelieres, 2006).

Clustering analysis

Protein clustering was measured as previously described (Saito *et al.*, 2012). Briefly, lines were drawn along cell borders to measure fluorescence intensity using ImageJ/Fiji (NIH, Bethesda, MD). A custom designed MATLAB program identified all local maxima (peaks) with an intensity at least half the maximum intensity. The clustering index is defined as 1 over the number of peaks per 5 μm distance.

Dispase-based fragmentation assay with immunofluorescence

Following PV IgG treatment, cells were subjected to a dispase fragmentation assay as previously described (Saito *et al.*, 2012). In parallel, cell sheets/fragments were fixed in paraformaldehyde, permeablized in Triton X-100 and incubated with primary and secondary antibodies in the tissue culture wells. Gentle washes with PBS^{+} were carried out between Triton and antibody incubations. Cell sheets/fragments were then mounted in ProLong Gold (Molecular Probes, Eugene, OR) and then imaged by SIM.

Statistics

Statistical analysis comparing the PV group to NH was performed using a *t*-test, assuming unequal variances with a significance level of $\alpha = 0.05$. For Figure 2b-c, pairwise multiple comparisons were performed via Holm-Sidak method with a significance level of $\alpha = 0.05$.

Supplementary Material

Refer to Web version on PubMed Central for supplementary material.

ACKNOWLEDGMENTS

We acknowledge members of the Kowalczyk laboratory for their insightful advice and discussions, and especially Ms. Susan Summers for keratinocyte isolations. We greatly appreciate the assistance of Ms. Bridget Bradley (Emory Dermatology) and Sue Manos (Emory Pathology) in obtaining and processing pemphigus patient samples. This work was conducted using funding and instrumentation made available through the Integrated Cellular Imaging Core (ICI) of Emory University. This work was supported by NIH R01AR048266 to APK and R21AR066920 to ALM. SNS was supported by NIH T32GM008367. MFW was supported by NIH UL1TR000454.

Abbreviations used

PV	pemphigus vulgaris
Dsg3	desmoglein 3
DP	desmoplakin
NH	normal human
IgG	antibodies

REFERENCES

Al-Jassar C, Bikker H, Overduin M, et al. Mechanistic basis of desmosome-targeted diseases. Journal of molecular biology. 2013; 425:4006–22. [PubMed: 23911551]

Amagai M. The molecular logic of pemphigus and impetigo: the desmoglein story. Veterinary dermatology. 2009; 20:308–12. [PubMed: 20178466]

Amagai M. Autoimmune and infectious skin diseases that target desmogleins. Proceedings of the Japan Academy Series B. Physical and biological sciences. 2010; 86:524–37. [PubMed: 20467217]

Amagai M, Karpati S, Prussick R, et al. Autoantibodies against the amino-terminal cadherin-like binding domain of pemphigus vulgaris antigen are pathogenic. The Journal of clinical investigation. 1992; 90:919–26. [PubMed: 1522242]

Berika M, Garrod D. Desmosomal adhesion in vivo. Cell communication & adhesion. 2014; 21:65–75. [PubMed: 24460202]

Bolte S, Cordelieres FP. A guided tour into subcellular colocalization analysis in light microscopy. Journal of microscopy. 2006; 224:213–32. [PubMed: 17210054]

Calkins CC, Setzer SV, Jennings JM, et al. Desmoglein endocytosis and desmosome disassembly are coordinated responses to pemphigus autoantibodies. The Journal of biological chemistry. 2006; 281:7623–34. [PubMed: 16377623]

Cirillo N. 150th anniversary series: desmosomes in physiology and disease. Cell communication & adhesion. 2014; 21:85–8. [PubMed: 24641511]

Cirillo N, Gombos F, Lanza A. Changes in desmoglein 1 expression and subcellular localization in cultured keratinocytes subjected to anti-desmoglein 1 pemphigus autoimmunity. Journal of cellular physiology. 2007; 210:411–6. [PubMed: 17058228]

Delva E, Jennings JM, Calkins CC, et al. Pemphigus vulgaris IgG-induced desmoglein-3 endocytosis and desmosomal disassembly are mediated by a clathrin- and dynamin-independent mechanism. The Journal of biological chemistry. 2008; 283:18303–13. [PubMed: 18434319]

Desai BV, Harmon RM, Green KJ. Desmosomes at a glance. Journal of cell science. 2009; 122:4401–7. [PubMed: 19955337]

Di Zenzo G, Di Lullo G, Corti D, et al. Pemphigus autoantibodies generated through somatic mutations target the desmoglein-3 cis-interface. The Journal of clinical investigation. 2012; 122:3781–90. [PubMed: 22996451]

Getsios S, Huen AC, Green KJ. Working out the strength and flexibility of desmosomes. Nature reviews Molecular cell biology. 2004; 5:271–81. [PubMed: 15071552]

Ishii K, Harada R, Matsuo I, et al. In vitro keratinocyte dissociation assay for evaluation of the pathogenicity of anti-desmoglein 3 IgG autoantibodies in pemphigus vulgaris. The Journal of investigative dermatology. 2005; 124:939–46. [PubMed: 15854034]

Iwatsuki K, Han GW, Fukuti R, et al. Internalization of constitutive desmogleins with the subsequent induction of desmoglein 2 in pemphigus lesions. The British journal of dermatology. 1999; 140:35–43. [PubMed: 10215765]

Iwatsuki K, Takigawa M, Imaizumi S, et al. In vivo binding site of pemphigus vulgaris antibodies and their fate during acantholysis. Journal of the American Academy of Dermatology. 1989; 20:578–82. [PubMed: 2469704]

Jennings JM, Tucker DK, Kottke MD, et al. Desmosome disassembly in response to pemphigus vulgaris IgG occurs in distinct phases and can be reversed by expression of exogenous Dsg3. The Journal of investigative dermatology. 2011; 131:706–18. [PubMed: 21160493]

Jolly PS, Berkowitz P, Bektas M, et al. p38MAPK signaling and desmoglein-3 internalization are linked events in pemphigus acantholysis. The Journal of biological chemistry. 2010; 285:8936–41. [PubMed: 20093368]

Kitajima Y. New insights into desmosome regulation and pemphigus blistering as a desmosome-remodeling disease. The Kaohsiung journal of medical sciences. 2013; 29:1–13. [PubMed: 23257250]

Kitajima Y. 150(th) anniversary series: Desmosomes and autoimmune disease, perspective of dynamic desmosome remodeling and its impairments in pemphigus. Cell communication & adhesion. 2014; 21:269–80. [PubMed: 25078507]

Kneisel A, Hertl M. Autoimmune bullous skin diseases. Part 1: Clinical manifestations. Journal der Deutschen Dermatologischen Gesellschaft = Journal of the German Society of Dermatology : JDDG. 2011; 9:844–56. quiz 57. [PubMed: 21955378]

Koga H, Tsuruta D, Ohyama B, et al. Desmoglein 3, its pathogenecity and a possibility for therapeutic target in pemphigus vulgaris. Expert opinion on therapeutic targets. 2013; 17:293–306. [PubMed: 23294403]

Kottke MD, Delva E, Kowalczyk AP. The desmosome: cell science lessons from human diseases. Journal of cell science. 2006; 119:797–806. [PubMed: 16495480]

Kowalczyk AP, Green KJ. Structure, function, and regulation of desmosomes. Progress in molecular biology and translational science. 2013; 116:95–118. [PubMed: 23481192]

Mao X, Li H, Sano Y, et al. MAPKAP kinase 2 (MK2)-dependent and -independent models of blister formation in pemphigus vulgaris. The Journal of investigative dermatology. 2014; 134:68–76. [PubMed: 23657501]

Mao X, Sano Y, Park JM, et al. p38 MAPK activation is downstream of the loss of intercellular adhesion in pemphigus vulgaris. The Journal of biological chemistry. 2011; 286:1283–91. [PubMed: 21078676]

Nekrasova O, Green KJ. Desmosome assembly and dynamics. Trends in cell biology. 2013; 23:537–46. [PubMed: 23891292]

North AJ, Bardsley WG, Hyam J, et al. Molecular map of the desmosomal plaque. Journal of cell science. 1999; 112(Pt 23):4325–36. [PubMed: 10564650]

Oktarina DA, van der Wier G, Diercks GF, et al. IgG-induced clustering of desmogleins 1 and 3 in skin of patients with pemphigus fits with the desmoglein nonassembly depletion hypothesis. The British journal of dermatology. 2011; 165:552–62. [PubMed: 21692763]

Patel HP, Diaz LA, Anhalt GJ, et al. Demonstration of pemphigus antibodies on the cell surface of murine epidermal cell monolayers and their internalization. The Journal of investigative dermatology. 1984; 83:409–15. [PubMed: 6389716]

Patel SD, Chen CP, Bahna F, et al. Cadherin-mediated cell-cell adhesion: sticking together as a family. Current opinion in structural biology. 2003; 13:690–8. [PubMed: 14675546]

Payne AS, Ishii K, Kacir S, et al. Genetic and functional characterization of human pemphigus vulgaris monoclonal autoantibodies isolated by phage display. The Journal of clinical investigation. 2005; 115:888–99. [PubMed: 15841178]

Saito M, Stahley SN, Caughman CY, et al. Signaling dependent and independent mechanisms in pemphigus vulgaris blister formation. PloS one. 2012; 7:e50696. [PubMed: 23226536]

Sato M, Aoyama Y, Kitajima Y. Assembly pathway of desmoglein 3 to desmosomes and its perturbation by pemphigus vulgaris-IgG in cultured keratinocytes, as revealed by time-lapsed labeling immunoelectron microscopy. Laboratory investigation; a journal of technical methods and pathology. 2000; 80:1583–92.

Schulze K, Galichet A, Sayar BS, et al. An adult passive transfer mouse model to study desmoglein 3 signaling in pemphigus vulgaris. The Journal of investigative dermatology. 2012; 132:346–55. [PubMed: 21956125]

Sekiguchi M, Futei Y, Fujii Y, et al. Dominant autoimmune epitopes recognized by pemphigus antibodies map to the N-terminal adhesive region of desmogleins. Journal of immunology. 2001; 167:5439–48.

Shapiro L, Weis WI. Structure and biochemistry of cadherins and catenins. Cold Spring Harbor perspectives in biology. 2009; 1:a003053. [PubMed: 20066110]

Sharma P, Mao X, Payne AS. Beyond steric hindrance: the role of adhesion signaling pathways in the pathogenesis of pemphigus. Journal of dermatological science. 2007; 48:1–14. [PubMed: 17574391]

Shimizu A, Ishiko A, Ota T, et al. IgG binds to desmoglein 3 in desmosomes and causes a desmosomal split without keratin retraction in a pemphigus mouse model. The Journal of investigative dermatology. 2004; 122:1145–53. [PubMed: 15140217]

Stahley SN, Kowalczyk AP. Desmosomes in acquired disease. Cell and tissue research. 2015

Stahley SN, Saito M, Faundez V, et al. Desmosome assembly and disassembly are membrane raft-dependent. PloS one. 2014; 9:e87809. [PubMed: 24498201]

Thomason HA, Scothern A, McHarg S, et al. Desmosomes: adhesive strength and signalling in health and disease. The Biochemical journal. 2010; 429:419–33. [PubMed: 20626351]

Tsunoda K, Ota T, Aoki M, et al. Induction of pemphigus phenotype by a mouse monoclonal antibody against the amino-terminal adhesive interface of desmoglein 3. Journal of immunology. 2003; 170:2170–8.

Tucker DK, Stahley SN, Kowalczyk AP. Plakophilin-1 protects keratinocytes from pemphigus vulgaris IgG by forming calcium-independent desmosomes. The Journal of investigative dermatology. 2014; 134:1033–43. [PubMed: 24056861]

van der Wier G, Pas HH, Kramer D, et al. Smaller desmosomes are seen in the skin of pemphigus patients with anti-desmoglein 1 antibodies but not in patients with anti-desmoglein 3 antibodies. The Journal of investigative dermatology. 2014; 134:2287–90. [PubMed: 24621791]

Vasioukhin V, Bowers E, Bauer C, et al. Desmoplakin is essential in epidermal sheet formation. Nature cell biology. 2001; 3:1076–85. [PubMed: 11781569]

Waschke J. The desmosome and pemphigus. Histochemistry and cell biology. 2008; 130:21–54. [PubMed: 18386043]

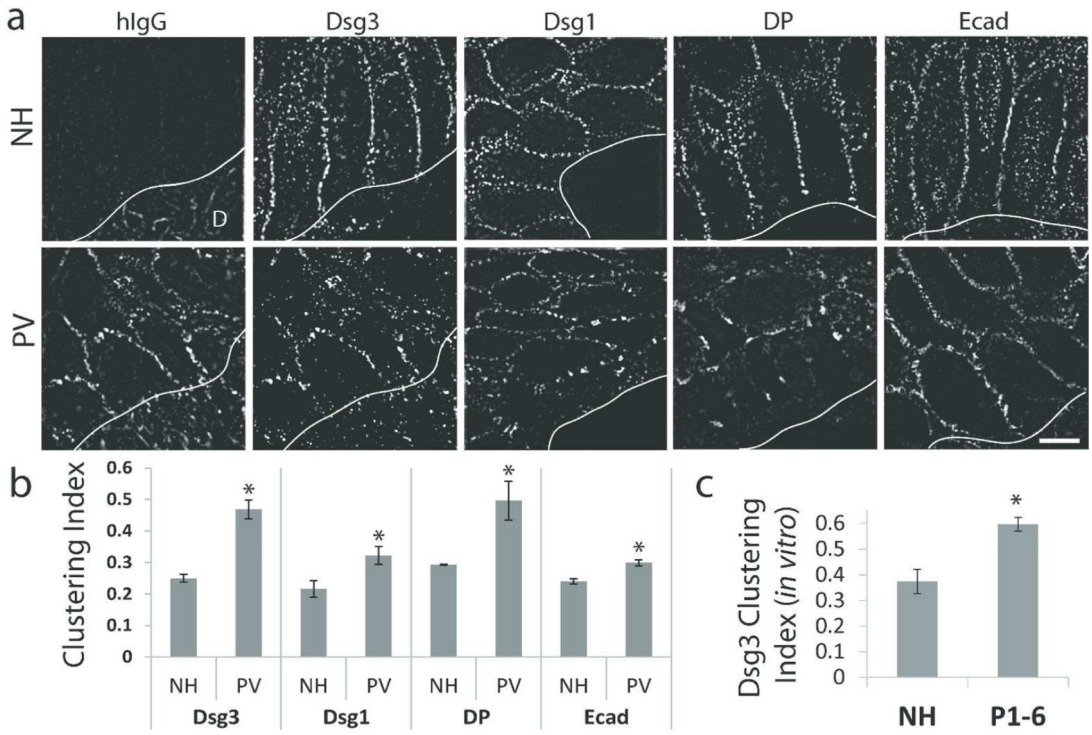

Figure 1. Desmosomal proteins are clustered in PV patients as assessed using SIM and immunofluorescence analysis

(a) Top panel: Normal human (NH) epidermal tissue is negative for IgG (hIgG) deposition and junctional proteins desmoglein 3 (Dsg3), desmoglein 1 (Dsg1), desmoplakin (DP) and E-cadherin (Ecad) are uniformly distributed along cell borders. Bottom panel: PV patient epidermis is positive for hIgG deposition and border localization of Dsg3, Dsg1 and DP is disorganized and clustered. Ecad staining is largely unaltered. D, dermis. Solid line, epidermis-dermis interface. Images oriented dermis down. Images from N1-3 and P1-2. Scale bar, 5 μm. **(b)** Quantification of protein clustering. Means ± SEM; *$p < 0.05$; Mean clustering index for each junctional protein represents data derived from 2-3 NH biopsies and 3-6 PV patient biopsies and the analysis of 135-850 μm of cell border length per patient. **(c)** Quantification of average Dsg3 clustering using purified patient IgG (P1-6) added to cultured keratinocytes. Means ± SEM; *$p < 0.05$; Mean clustering index was derived from 765-1830 μm of cell border length per IgG sample.

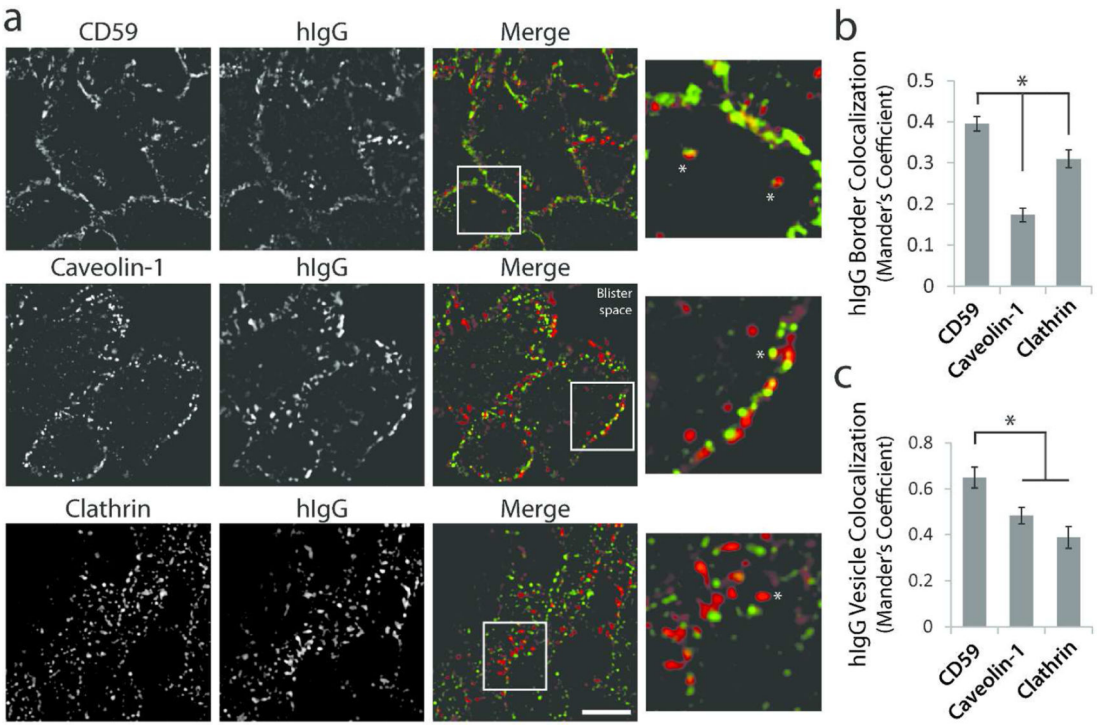

Figure 2. PV patient IgG colocalizes with lipid raft markers *in vivo*

(a) Colocalization of PV patient IgG (hIgG) with lipid raft markers CD59 (top panel) and caveolin-1 (middle panel), and non-raft marker clathrin (bottom panel) in biopsies from PV patient tissue. Colocalization is observed both at cell borders and in vesicular-like structures (asterisks). Note lack of clathrin colocalization in vesicular puncta. Images from P5. Scale bar, 5 μm. **(b)** Quantification of hIgG colocalization (Mander's coefficient) with membrane markers at cell-cell borders. Means ± SEM, *$p < 0.05$; n = at least 54 cell borders from biopsies derived from 3 different patients. **(c)** Quantification of vesicular hIgG colocalization (Mander's coefficient) with membrane markers. Means ± SEM; *$p < 0.05$; n = 30 vesicles analyzed from three patient biopsies.

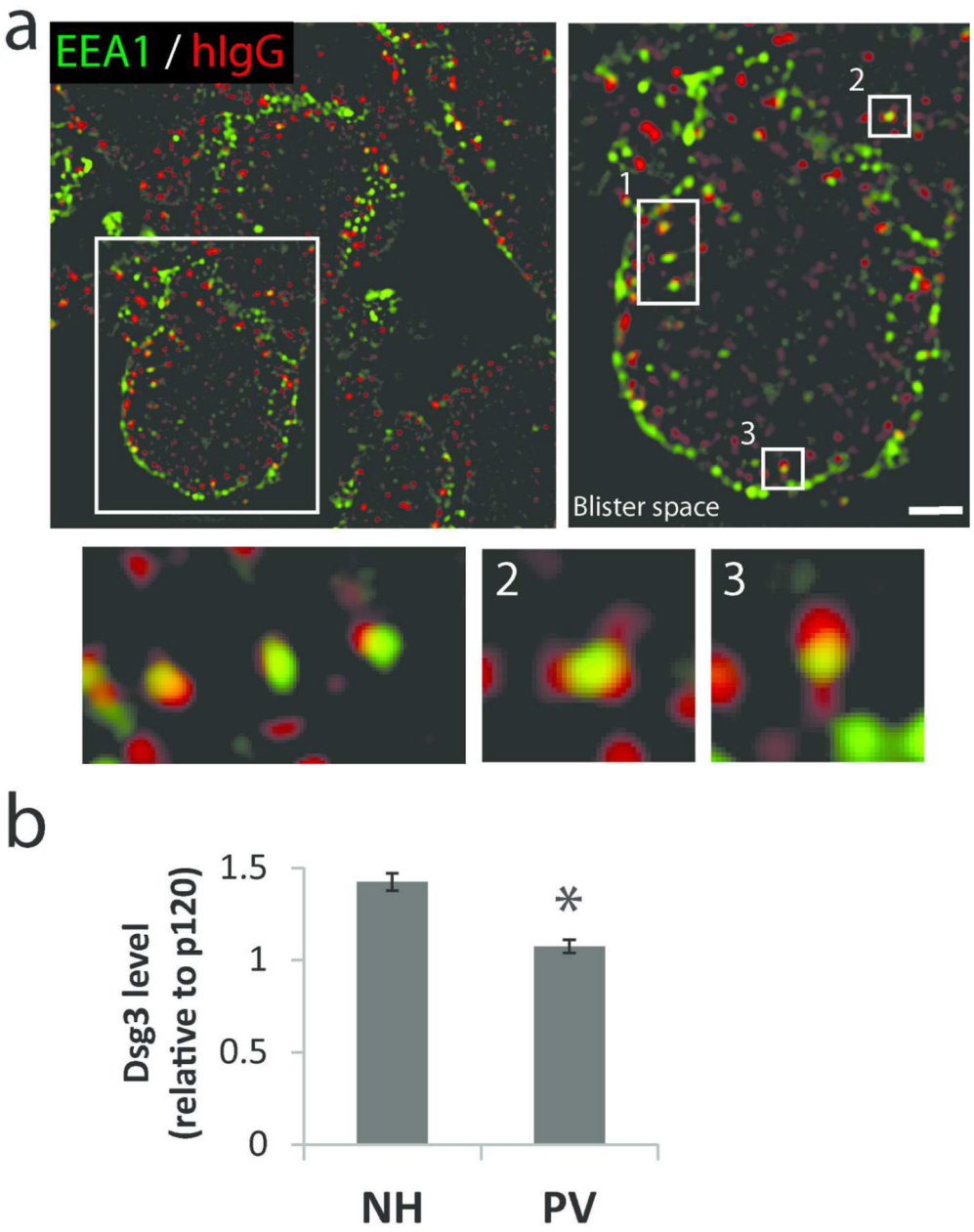

Figure 3. PV patient IgG is internalized *in vivo* and Dsg3 levels are reduced

(a) PV IgG (hIgG) colocalizes with early endosomal marker EEA1. Numbered enlargements highlight vesicular colocalization. Images from P5. Scale bar, 2 μm. **(b)** Quantification of Dsg3 protein levels relative to adherens junction protein p120 in normal and PV patient tissue. Image J was used to analyze wide-field microscopy images of tissue. Following background subtraction, Dsg3 intensity was normalized to p120 levels using Image J. Means ± SEM; *$p < 0.05$; Data were collected from 3 NH and 5 PV patient biopsies. Average fluorescence intensity measurements were derived from analysis of 6-10 images from each biopsy.

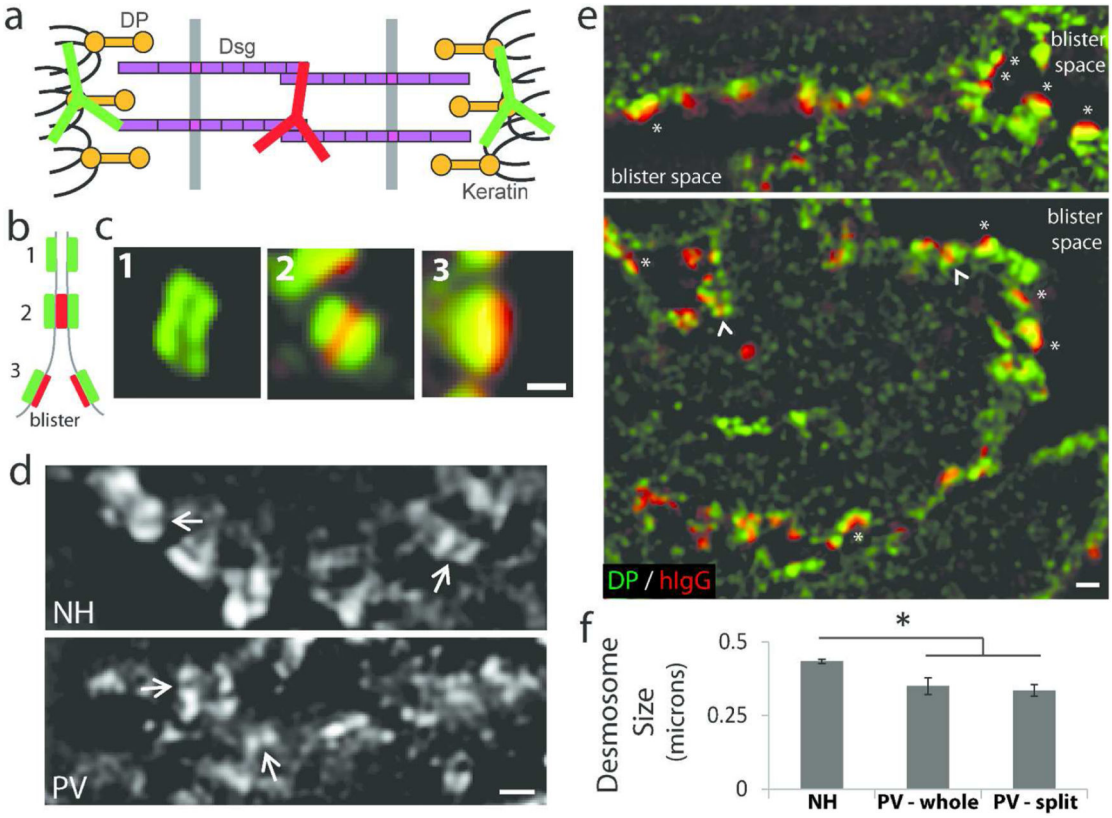

Figure 4. Desmosomes in PV patients are smaller and split

(a) Desmosome schematic depicting staining with N-terminal Dsg3 antibody (hIgG in patient tissue) and a C-terminal desmoplakin (DP) antibody. **(b)** SIM resolves the plaque to plaque distance and desmosomes appear as regions of parallel DP staining, or 'railroad' tracks, along a cell border (1) or a sandwich of DP-Dsg3-DP staining (2). Split desmosomes appear as regions of green-red staining (3). **(c)** *In vivo* examples of (b). Scale bar, 0.3 μm. **(d-f)** Normal human (NH) and PV patient biopsies stained as detailed above and imaged by SIM. Railroad tracks were used to identify and measure desmosome size. **(d)** DP staining. Arrows indicating intercellular space highlight smaller desmosomes. Images from N3 and P1. Scale bar, 0.5 μm. **(e)** Many split (or half) desmosomes with IgG staining (asterisks) are observed adjacent to the blister space. Small desmosomes (arrowheads) were also observed. DP (green), hIgG (red). Images from P5. Scale bar, 0.5 μm. **(f)** Quantification of desmosome size. Means ± SEM; * $p < 0.05$ comparing PV-whole or PV-split to NH; measurements were obtained from 6-163 desmosomes per patient; data from three NH controls and six PV patients.

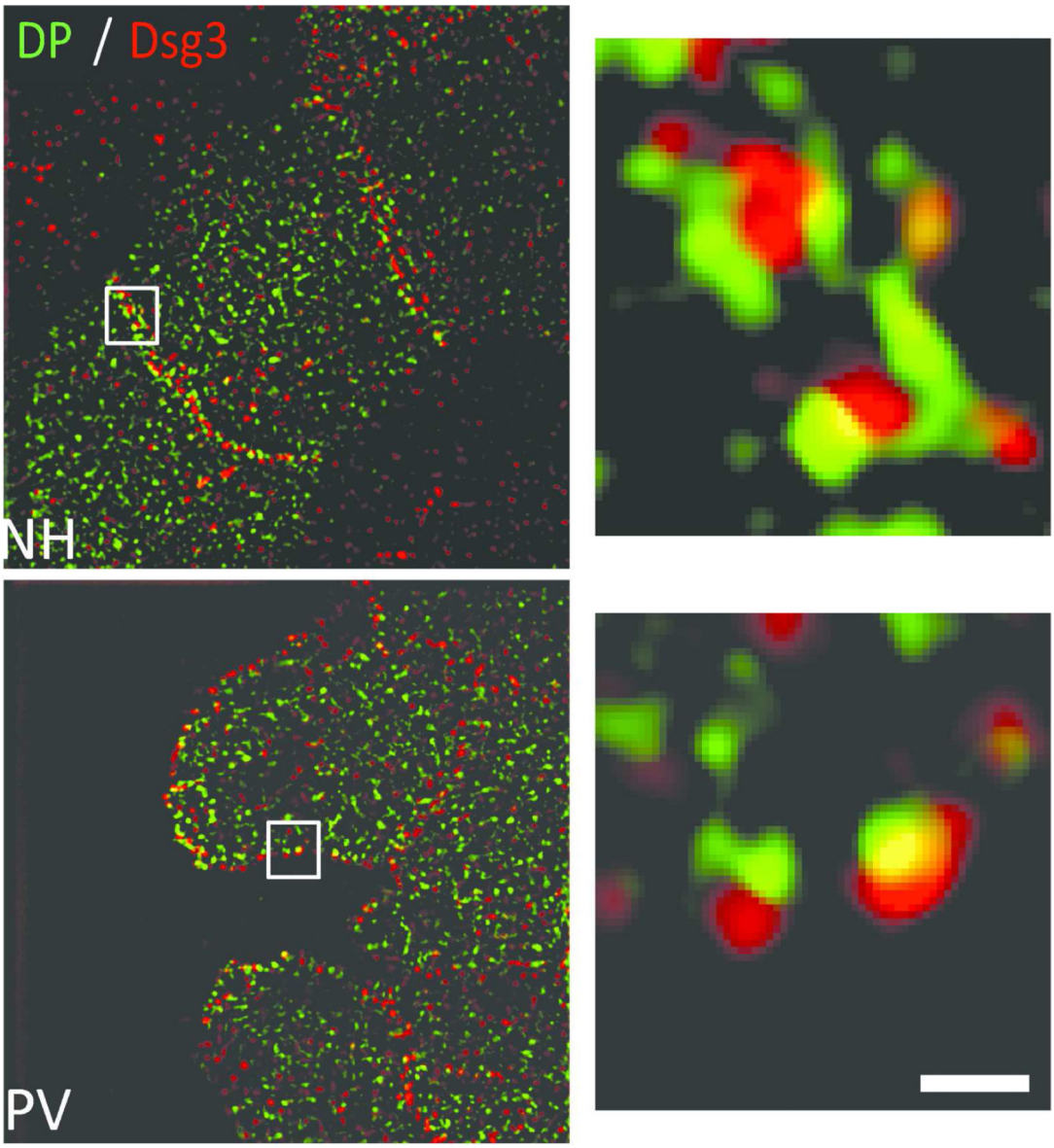

Figure 5. Mechanical stress causes desmosome splitting in cultured keratinocytes exposed to PV IgG

Keratinocyte monolayers exposed to either normal human (NH) or PV IgG were subjected to mechanical stress by repeated pipetting and then processed for SIM. The keratinocyte sheet exposed to NH IgG display intact desmosomes at cell borders indicated by the green-red-green 'rail-road' track staining pattern (top panel). The free edge of the fragmented sheet exposed to PV IgG exhibits multiple split desmosomes (bottom panel) indicated by only a green-red staining. Scale bar, 0.5 μm.